RSC Advances

PAPER

View Article Online
View Journal | View Issue

Cite this: *RSC Adv.*, 2014, **4**, 3096

Two novel macrocyclic organotin(IV) carboxylates based on amide carboxylic acids†

Xiao Xiao,[a] Lisong Yan,[b] Zemin Mei,[c] Dongsheng Zhu*[a] and Lin Xu[a]

Received 29th October 2013
Accepted 2nd December 2013

DOI: 10.1039/c3ra46198j

www.rsc.org/advances

Two novel macrocyclic organotin(IV) carboxylates $[(n\text{-}Bu_2Sn)L^1]_2{\cdot}C_7H_8$ (**1**) (L^1 = 2-(4-carboxyphenylcarbamoyl)benzoic acid) and $[(n\text{-}Bu_2Sn)L^2]_3{\cdot}H_2O$ (**2**) (L^2 = 5-(1,3-dioxo-1,3-dihydro-isoindol-2-yl)-isophthalic acid) were generated by the reactions of dibutyltin oxide with amide dicarboxylic acids and characterized by elemental analysis, IR, ^1H and ^{13}C NMR spectroscopy. X-ray crystallography diffraction analyses reveal that **1** is a di-nuclear dicarboxylate ring and **2** is a trinuclear tricarboxylate macrocycle. With the help of intermolecular interactions, **1** and **2** construct supramolecular 3D architectures filled with cavities. Free toluene and water molecules are located in the cavities of **1** and **2** respectively as guests. Thermal analyses suggest that complex **2** is thermally more stable than **1**. The antitumour activity of **1** and **2** has also been studied.

Introduction

The molecular constructions with cavities or possessing intrinsic physical properties have the potential to create new materials.[1a] The supramolecular class possessing cavities can be used for molecular recognition, storage, absorption, separation, host–guest system and polymeric structures with voids or channels are available for the inclusion of guest molecules.[1] However, compared to the transition metals and lanthanides, few supramolecular polymers containing main group elements have been studied.[1a,2]

Macrocyclic organotin carboxylates are attractive for these reasons. Although receiving attention, the relevant reports are numbered.[3] To further the field of organotin carboxylate macrocycle with esthetic architecture and to explore the rules of molecular ring formation, we suppose to synthesize novel organotin carboxylate macrocycle with fascinating supramolecular structure.

As we know, metal–ligand binding, hydrogen bonds and $\pi\cdots\pi$ interactions play key roles for the generation of infinite number of supramolecular entities with intra- and intermolecular cavities.[4] We chose two amide dicarboxylic acids (L^1 and L^2) as ligands for following reasons: (a) dicarboxylic acid providing various bridging abilities and strong coordination tendency with metals inducing rich coordination modes, interesting molecular macrocyclic composition and supramolecular structure; (b) different constructions of them which will help us study the relation of them and the structure of produced complex; (c) flexible L^1 and rigid L^2 inclined to cause different rigidity of 2- and 3D networks. Based on the above, di-nuclear centrosymmetric dicarboxylate **1** and trinuclear tricarboxylate macrocycle **2** are obtained through the reactions of L^1 and L^2 with Bu_2SnO respectively. By the search of CSD, we found that macrocyclic organotin complexes are less studied, much of which are tri-, tetra-, and hexanuclear.[5] The reports about di-nuclear dicarboxylate macrocycle are fewer, while **1** has the dimeric structure of macrocycle with two tin centers. *Via* intermolecular interactions, **1** and **2** form 3D supramolecular architectures with intermolecular cavities occupied by free toluene and water molecules respectively.

Results and discussion

Synthesis

Through the reaction of $(n\text{-}Bu)_2SnO$ and ligand (L^1 and L^2), **1** and **2** are obtained (Scheme 1). From the structure analyses of complexes **1** and **2**, it can be concluded that $(n\text{-}Bu)_2SnO$ reacting with dicarboxylic acid (L^1 and L^2) is apt to produce expected organotin carboxylate with macrocycle structure. And different structure of the ligand will lead different construction of the macrocycle. The reaction of $(n\text{-}Bu)_2SnO$ with L^1 tends to produce ring with two metal centers. When with L^2, it inclines to form ring with three nucleus. Meanwhile, the number of ligands participating in ring formation changes with that of the tin centers.

[a]*Northeast Normal University, Department of Chemistry, Changchun, China. E-mail: zhuds206@nenu.edu.cn; Fax: +86 0431 85684009; Tel: +86 0431 85098620*

[b]*Changchun Institute of Optics Fine Mechanics and Physics Chinese Academy of Sciences, Key Laboratory of Optical System Advanced Manufacturing Technology, Changchun, China*

[c]*Baicheng Normal University, Department of Chemistry, Baicheng, China*

† Electronic supplementary information (ESI) available: Antitumor activity experiment; selected bond lengths (Å) and angles (°) for complexes **1** and **2**; crystal data for **1** and **2**; TGA-DTG curves of **1** and **2**; Inhibition effects of **1**, **2**, L^1 and L^2 against S180. CCDC 827597 and 827595. For ESI and crystallographic data in CIF or other electronic format see DOI: 10.1039/c3ra46198j

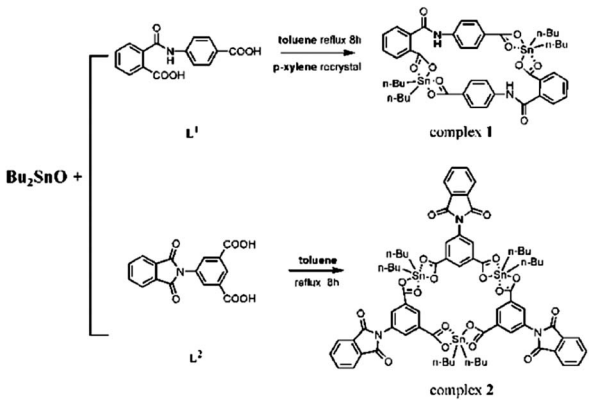

Scheme 1 Syntheses of complexes **1** and **2**.

Molecular structure

Complex 1. The molecular structure of complex **1** is shown in Fig. 1(a). Selected bond lengths and angles are listed in Table S1.† The unit cell includes a dinuclear tin ring and a free toluene molecule. The complex lies about an inversion centre and the free toluene lies disordered about another inversion centre. **1** is a symmetric 26-membered dinuclear macrocycle with an inversion center. The macrocycle is linked by *n*-Bu_2Sn groups and ligands L^1 alternately. Two tin atoms are hexa-coordinated by two carbon atoms of *n*-butyl moieties in the axial site and four carboxylate oxygen atoms of L^1 occupying the equatorial plane. The axial angle of C–Sn–C is 144.86(13)° and the O–Sn–O angles around tin are 55.57(7)° [O(3)–Sn(1)–O(1)] and 56.15(8)° [O(4)–Sn(1)–O(2)], which are commonly observed for diorganotin carboxylate.[6] For the tension of ring formation, each ligand L^1 binds to two tin atoms by two types of Sn–O bond distances: short Sn–O distance [Sn(1)–O(3): 2.152(2) Å; Sn(1)–O(4): 2.118(2) Å] and long Sn–O distance [Sn(1)–O(1): 2.503(2) Å; Sn(1)–O(2): 2.507(2) Å], which prove the anisobidentate chelating coordination mode of the carboxylate groups. The long Sn–O distance is much shorter than the sum of the van der Waals radii of tin and oxygen (3.7 Å)[7a] which indicates a strong coordinating bond. These Sn–O and relative Sn–C [2.114(3) and 2.118(3) Å] bond lengths may be compared with those found in the analogous complex $[(n\text{-}Bu)_2SnFc(CO_2)_2]_2$.[5d] Thus the coordination environment of Sn can be described as a distorted octahedron [Fig. 1(b)]. The ring demonstrates as a twisty rectangle with the benzene rings [IA and IIA, IB and IIB in Fig. 1(a)] paralleled. Distance between two tin centers is calculated as 9.950 Å. The cross section of the cavity is probable 11.958 Å × 5.561 Å which is larger than those reported in $[(n\text{-}Bu)_2SnFc(CO_2)_2]_2$ and $[Bn_2SnFc(CO_2)_2]_2$.[5d]

The dinuclear macrocyclic rings in the crystal lattice are linked into 1D polymeric chains through an extensive set of weak intermolecular Sn(1)···O(1) interactions [Fig. 2(a)]. These Sn···O interactions (3.066 Å) give rise to the formation of a Sn_2O_2 distannoxane unit [Sn(1)···O(1)···Sn(1)···O(1) 2.503 Å × 3.066 Å]. The unit demonstrates as a parallelogram evidenced by the O–Sn–O bond angle 64.83° and Sn–O–Sn bond angle 115.17°. Considering these Sn···O interactions, the coordination geometry of tin atom is best described as a skew-pentagonal bipyramid [Fig. 2(b)]. The 1D chain links with other four *via* N–H(1A)···O(5) (2.151 Å) hydrogen bonds along four different directions. Two locate below and two upon the chain [Fig. 2(a)]. Both the hydrogen and oxygen atoms involved in the N–H···O interactions belong to the imide group. Through this kind of connections, intermolecular channel is formed by four chains [Fig. 3(a)]. Each two on the opposite sides of the chains are almost paralleled. Toluene guest resides inside the channel and is stabled by C–H···π interactions (Fig. S1†). In Fig. 3(b) the macrocyclic molecule is simplified into a dark green sphere for clarity. The red bonds stand for Sn···O interactions and green ones are representative of N–H···O bonds. These connections help the molecules construct 3D cages locking guest toluene molecules in.

Complex 2. The molecular structure of complex **2** is shown in Fig. 4. Sn(2), N(2) and C(25) atoms lie on the twofold axis in this structure. Selected bond distances and angles are listed in Table S1.† The trinuclear tin complex is symmetric with a two-fold axis and characterized by a 24-membered $C_{15}O_6Sn_3$ macrocyclic ring system with all six oxygen atoms directed into the interior of the cavity. Six *n*-butyl groups attached to the tin centers are three below and three upon the ring. Sn(1) adopts distorted trigonal bipyramidal coordination geometry. It is five coordinated by three O atoms from carboxylate groups of L^2 and two *n*-Bu groups. The C–Sn–C angle of Sn(1) is 160.82(4)°. It can be seen from Fig. 4 that one L^2 coordinates with Sn(1) by monodentate

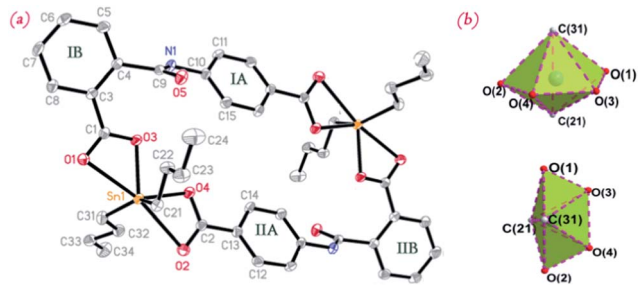

Fig. 1 (a) Molecular structure of **1** (30% probability displacement ellipsoids). (b) Coordination polyhedron of Sn.

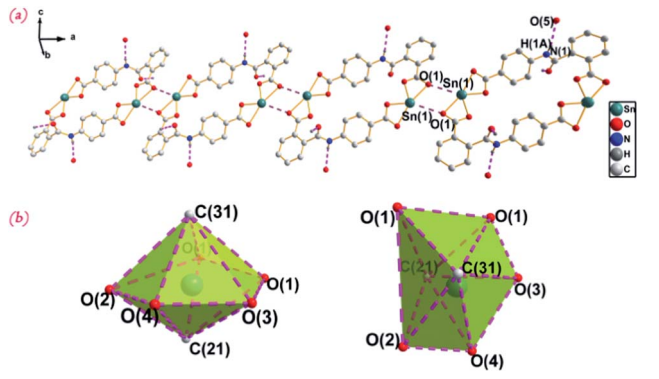

Fig. 2 (a) Supramolecular 1D chain structure of **1**. Butyl groups are omitted for clarity. (b) Coordination polyhedron concerning intermolecular Sn···O interaction of Sn.

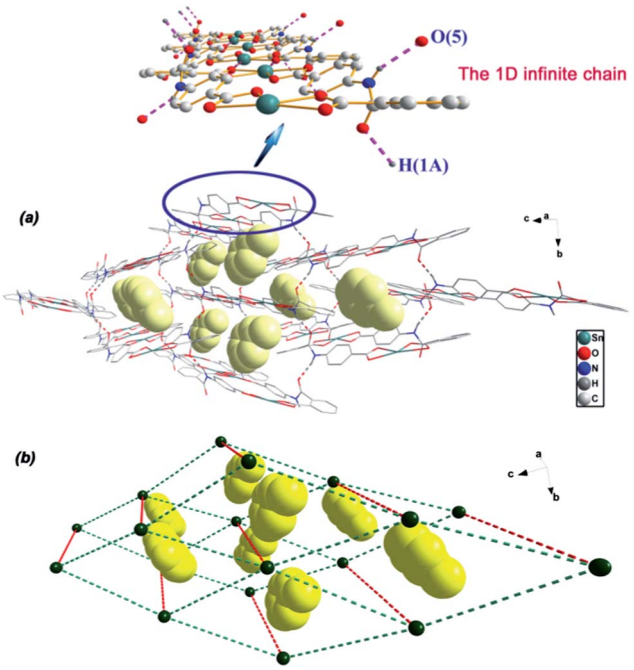

Fig. 3 Supramolecular 3D structure of **1**.

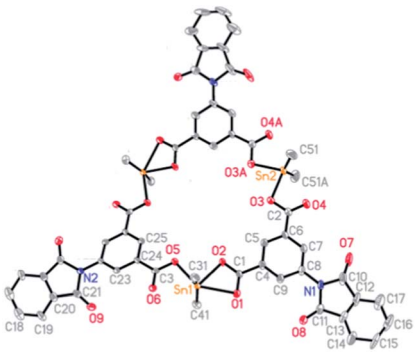

Fig. 4 Molecular structure of **2** (30% probability displacement ellipsoids). Part of butyl groups are omitted for clarity. "A" indicates atoms at equivalent position ($1 - x, y, -1/2 - z$).

mode with Sn–O bond length 2.170(5) Å. Another L^2 adopts bidentate chelating mode as complex **1** with two kinds of Sn–O bond lengths [Sn(1)–O(1): 2.390(5) Å; Sn(1)–O(2): 2.173(5) Å]. Sn(2) is different from Sn(1) for that both of the coordinated ligands use monodentate coordination mode with Sn–O distance 2.107(6) Å. Thus Sn(2) has a distorted tetrahedron configuration coordinated by two carboxylate O atoms and two C atoms from butyl groups. For the tremble of *n*-Bu groups, the C–Sn–C angle of Sn(2) is 141.2(8)°, which also makes Sn(2) difficult to chelate with other atoms. Besides the coordination bonds mentioned above, the distances of Sn(1)···O(6) (2.680 Å) and Sn(2)···O(4) (2.568 Å) lie in the range of intramolecular Sn–O bond distances.[7b] Therefore the oxygen atoms [O(4) and O(6)] are involved in a weak coordinative interaction with tin and all tin centers can be considered as hexa-coordinated with a skewed trapezoidal bipyramid configuration. O–Sn–O angles of Sn(1) and Sn(2) are among 52.67–57.49°. The cross section of the cavity can be evaluated by alternant Sn···Sn and O···O [O(2)···O(3), O(2A)···O(3A), O(5)···O(5A)] distances, which are among 9.02–9.14 and 4.86–4.94 Å, respectively.

Interestingly, intermolecular Sn···O coordinations [Sn(1)···O(6A) and Sn(1A)···O(6)] with relative short distance 2.61 Å are observed in the crystal lattice. The rigid macrocyclic ring in the complex is squeezed as a twisty dimensional triangle for these strong intermolecular coordinations (Fig. S2 and S3†). This torsion and intermolecular Sn···O coordination is rare for the rigid tri-nuclear macrocyclic organotin.[1a,b,5c,6f,7c] The intermolecular Sn···O coordinations connect the rings and form intermolecular distannoxane units [Sn(1)···O(6)···Sn(1A)···O(6A)] [Fig. 5(a)]. The units are parallelogram proved by the O–Sn–O and Sn–O–Sn bond angles 68.11° and 111.89° respectively. The width of this type of units (2.61 Å × 2.68 Å) is close to that in **1**. Considering this type of interaction, the coordination environment of Sn(1) can also be regarded as distorted bipyramidal-pentagon [Fig. 5(b)]. And the molecular cyclic rings are linked into a one-dimensional zig-zag chain along *c* axis *via* these interactions [Fig. 5(d)].

Intermolecular hydrogen bonds help the chains connect with each other and form the supramolecular 3D architecture. As shown in Fig. 6(a), two kinds of hydrogen bonds C(16)–H(16A)···O(5) (2.57 Å) and C(15)–H(15A)···O(2) (2.58 Å) extend every chain into four different spatial orientations (two up and two below the chain) and construct the supramolecular 3D architecture of **2**. Intermolecular channels are formed by four chains linked with the hydrogen bonds as complex **1**. In Fig. 6(b), the supramolecular 3D structure with intermolecular channels serve as host and the guest water molecules are located in the channels disorderly.

IR, ^{1}H, and ^{13}C NMR spectra

In the IR spectra of **1** and **2**, a broad band in the region 3400–2800 cm^{-1} owing to the COOH group of ligands L^1 and L^2 is absent, which indicates the deprotonation of the carboxylic acid and metal–ligand bond formation through these sites.[7d] The $\Delta\nu$ ($\nu_{asym}COO - \nu_{sym}COO$) value for complex **1** is 144 cm^{-1} smaller

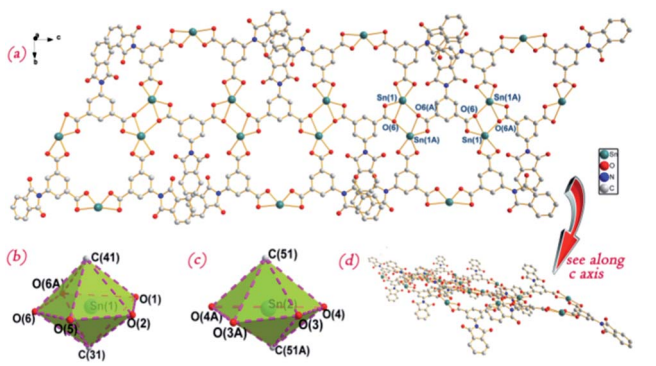

Fig. 5 (a) 1D chain structure of **2**. Butyl groups are omitted for clarity. (b) Coordination polyhedron concerning intermolecular Sn···O coordination of Sn(1). (c) Coordination polyhedron of Sn(2). (d) 1D chain structure of **2** along *c* axis.

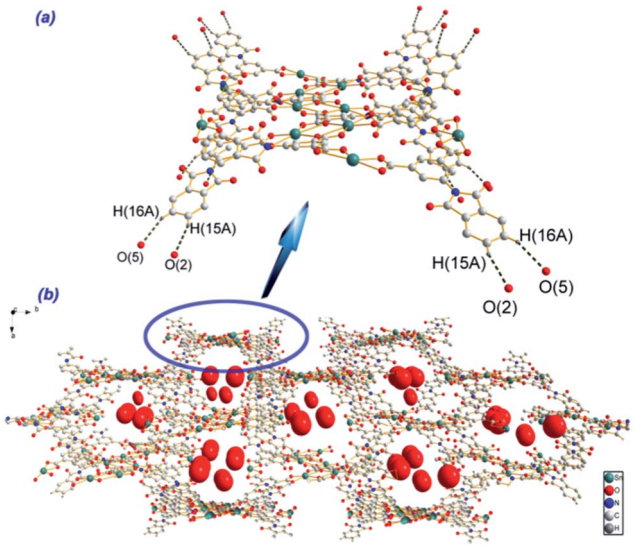

Fig. 6 Supramolecular 3D structure of **2**.

than 200 cm^{-1}, indicative of the bidentate chelating mode for the carboxyl ligand L^1. For **2**, the values are 195 and 210 cm^{-1}, which are representative of that both monodentate and bidentate coordinating modes exist in **2**.[2a,3b,d] These are totally consistent with the X-ray structures. The bands at 564 and 556 cm^{-1} for **1** and **2** respectively are assigned to the stretching frequency associated with the Sn–C bond. Strong bands of 459 and 467 cm^{-1} are assigned to ν(Sn–O), indicating the Sn–O coordinated structure.[4c,7e]

The ^{1}H NMR spectra show that the signals of the –COOH proton in ligands are absent in **1** and **2**, standing for the removal of –COOH proton and the formation of Sn–O bond.[3b,5b] Expected integration and peak multiplicities for the hydrogen protons on aromatic rings of ligands are observed in 7.65–9.10 ppm range. The chemical shift for "–NH–" group of L^1 in **1** is at 7.92 as single peak.[7e] Signals for the hydrogen protons on butyl groups of tin can also be appropriately attributed.

In the ^{13}C NMR spectra, Single resonances at 172.31 and 174.66 ppm of **1** and **2** are assigned to COO groups, and the ones at 167.25 and 166.79 ppm are owing to C=O groups.[2a,3b,7e] The peaks of aromatic rings and butyl groups can be appropriately attributed. The tin–carbon coupling constants $^1J_{^{119}Sn-^{13}C}$ are 778 and 801 Hz for **1** and **2**; on the basis of Holecek and Lycka equation,[8a,b] the C–Sn–C angles are estimated to 145° and 147° respectively, which agrees well with the coordination geometry around tin atoms in X-ray crystallography diffraction analyses.

Thermal analysis

Thermal analyses of **1** and **2** were studied by TGA and DTG (Fig. S4 and S5†). According to the DTG, it is observed that complexes **1** and **2** decompose in two steps.[8c,d] Complex **1** shows a gradual weight loss until 293 °C (weight loss of 8.60% is identical with a free toluene molecule). Continued two-step decomposition is revealed between 293 °C and 507 °C. With the weight loss of 62.57% which are accorded with two ligands and four *n*-Bu groups, 28.83% residual mass is observed. **2** exhibits a weight loss of 1.99% in the range of 50–365 °C, which agrees with the calculated value of free water molecule. Successive two-step decomposition is observed in the temperature range 365–490 °C. 60.90% weight loss in 365–800 °C is consistent with three ligands and six *n*-Bu groups. Thus, the final percentage of residual mass observed is 37.11%. From the above, it can be concluded that complex **2** is thermally more stable than **1**. There is virtually no weight loss until 365 °C.

Antitumor activity

The cell cytotoxicity of **1**, **2**, L^1 and L^2 against mouse sarcoma cells S180 was studied by MTT assays. The inhibition effects of them are shown in Fig. S6.† It can be seen that the growth rates of S180 are 39.46%, 37.15%, 81.49% and 85.75% after being added with test samples **1**, **2**, L^1 and L^2 respectively. And the relative inhibition ratios of them are 60.54%, 62.85%, 18.51% and 14.25%. L^1 gives higher cell cytotoxicity than L^2, while complex **1** exhibits a little lower antitumor activity than **2**. Due to very low cytotoxicity of the ligands, the complexation of these ligands with Sn(IV) has great contribution to the antitumor activity of the compounds. Generally the high antitumor activity shows the potential of complexes **1** and **2** in being used as an anticancer drug for chemotherapy.

Conclusion

In summary, we have synthesized and characterized two unique macrocyclic organotin carboxylates based on amide carboxylic acids. **1** has the rare structure of macrocycle with two tin centers. **2** is a trinuclear tricarboxylate ring. With the help of intermolecular interactions, **1** and **2** form attractive 3D supramolecular architectures with cavities. Free toluene and water molecules are situated in the intermolecular cavities of **1** and **2** as guest. Their structures which can serve as host–guest system help us further understand the group of organotin carboxylates. Moreover, it is interesting that Bu_2SnO reacts with dicarboxylic amide acids with different structures resulting different constructions of the macrocycle: with L^1, the reaction produces ring with two tin centers; with L^2 it forms ring with three nucleus. This provides an exploration and an effective exemplification for projecting the structure of ligand to change the macrocyclic composition of organotin carboxylate and consequently adjust the width of molecular cavity.

Experimental section

Materials and measurements

Di-*n*-butyltin oxide and L^1 are commercial available and was used without further purification. L^2 was prepared by a modified literature method.[9a] The solvents were purified according to standard procedures before used.[9b] The melting point was obtained with Kofler micro-melting point apparatus and was uncorrected. Elemental analysis (C, H, N) was carried out on a Perkin-Elmer PE 2400 CHN instrument. IR spectrum (KBr pellets) was recorded on an Alpha Centauri FI/IR spectrometer

(400–4000 cm^{-1} range). ^1H, ^{13}C NMR spectra were recorded on Varian Mercury operating at 300 and 75 MHz, respectively. The thermostability of **1** and **2** was measured on a Q500 TGA thermogravimetric analyzer (V6.5 Build 196).

X-ray crystallography

Diffraction intensities for complex **1** and **2** were collected on a Bruker CCD Area Detector image plate diffractometer by using the ω/φ scan technique with Mo-Kα radiation (λ= 0.71073 Å). Absorption corrections were applied by using multiscan techniques. The structure was solved by direct methods with SHELXS-97 (ref. 9*c*) and refined using SHELXL-97.[9*d*] All non-hydrogen atoms were refined with anisotropic temperature parameters; hydrogen atoms were refined as rigid groups. Crystal data for **1** and **2** are listed in Table S2.†.

Synthesis of $[(n\text{-}Bu_2Sn)L^1]_2\cdot C_7H_8$ (1)

A solution of L^1 (0.285 g, 1.0 mmol) and di-*n*-butyltin(IV) oxide (0.249 g, 1.0 mmol) in toluene (50 ml) was refluxed for 8 h using a Dean–Stark trap to facilitate the dynamic removal of the water formed in the reaction by azeotropic distillation. After cooling to room temperature, the solvent mixture was filtrated. The filtrate was allowed to slow evaporation of toluene at room temperature to afford white powder. Recrystallization of the powder with toluene produces colourless crystals of complex **1**. Yield: 68.2%, 0.38 g. Mp: >300 °C. Anal. calcd for $C_{45}H_{51}N_2O_{10}Sn_2\cdot C_7H_8$: C, 56.29; H, 5.36; N, 2.52. Found: C, 56.78; H, 5.39; N, 2.55%. IR (cm^{-1}): 1662 [s, ν (O=C)]; 1594 [s, ν_{asym}(COO)]; 1450 [s, ν_{sym}(COO)]; 564 [m, ν(Sn–C)]; 459 [s, ν(Sn–O)]. ^1H NMR ($CDCl_3$): δ 8.02–8.08 (m, 8H, Ar-H), 7.92 (s, 2H, –NH–), 7.79 (d, 4H, J = 7.6 Hz, Ar-H), 7.65 (d, 4H, J = 7.6 Hz, Ar-H), 1.63 (t, 8H, J = 6.7 Hz, Bu-H), 1.25–1.36 (m, 16H, Bu-H), 0.81 (t, 12H, J = 6.9 Hz, Bu-H). ^{13}C NMR ($CDCl_3$): δ 172.31 (4C, COO), 167.25 (2C, C=O), 142.72 (2C, Ar-C: C10), 135.12 (2C, Ar-C: C4), 134.23 (2C, Ar-C: C6), 131.76 (2C, Ar-C: C7), 130.27 (4C, Ar-C: C12, C14), 130.14 (2C, Ar-C: C8), 129.04 (2C, Ar-C: C3), 128.23 (2C, Ar-C: C5), 126.46 (2C, Ar-C: C13), 123.56 (4C, Ar-C: C11, C15), 26.57 (4C, Bu-C: $-CH_2-$), 25.26 (4C, Bu-C: $-CH_2-$), 13.48 (4C, Bu-C: $-CH_3$), 8.76 (4C, $^1J_{^{119}Sn-^{13}C}$ = 778 Hz, Bu-C: Sn–CH_2-).

Synthesis of $[(n\text{-}Bu)_2Sn(L^2)]_3\cdot H_2O$ (2)

The synthesis of **2** is similar to that of **1** except that L^2 (0.311 g, 1.0 mmol) was used to take place of L^1. And the crystals of **2** suitable for X-ray analysis are obtained directly by slow evaporation of toluene at room temperature without recrystal. Yield: 61.4%, 0.34 g. Mp: > 300 °C. Anal. calcd for $C_{72}H_{75}N_3O_{18}Sn_3H_2O$: C, 52.58; H, 4.72; N, 2.56. Found: C, 52.18; H, 4.68; N, 2.61%. IR (cm^{-1}): 1732 [s, ν(O=C)]; 1618, 1575 [s, ν_{asym}(COO)]; 1423, 1365 [s, ν_{sym}(COO)]; 556 [m, ν(Sn–C)]; 467 [s, ν(Sn–O)]. ^1H NMR ($CDCl_3$): δ 9.10 (s, 3H, Ar-H), 8.45 (s, 6H, Ar-H), 8.01 (d, 6H, J = 7.1 Hz, Ar-H), 7.85 (dd, 6H, J = 7.1 Hz, Ar-H), 1.71 (t, 12H, J = 6.9 Hz, Bu-H), 1.37–1.45 (m, 24H, Bu-H), 0.91 (t, 18H, J = 6.5 Hz, Bu-H). ^{13}C NMR ($CDCl_3$): δ 174.66 (6C, COO), 166.79 (6C, C=O), 134.74 (3C, Ar-C: C8, C22), 133.31 (6C, Ar-C: C12, C13, C20), 132.13 (6C, Ar-C: C15, C16, C18), 131.94 (6C, Ar-C: C4, C6, C24), 131.68 (6C, Ar-C: C14, C17, C19), 131.56 (3C, Ar-C: C5, C25), 124.03 (6C, Ar-C: C7, C9, C23), 26.61 (6C, Bu-C: $-CH_2-$), 26.02 (6C, Bu-C: $-CH_2-$), 13.54 (6C, Bu-C: $-CH_3$), 7.35 (6C, $^1J_{^{119}Sn-^{13}C}$ = 801 Hz, Bu-C: Sn–CH_2-).

Acknowledgements

We acknowledged the Science and technology department of Jilin province (no. 20120440).

Notes and references

1 (*a*) R. G. Zarracino and H. Höpfl, *J. Am. Chem. Soc.*, 2005, **127**, 3120; (*b*) A. G. Davies, M. Gielen, K. H. Pannell and E. R. T. Tiekink, *Tin Chemistry – Fundamentals, Frontiers, and Applications*, 1st edn, 2008; (*c*) R. Trokowski, S. Akine and T. Nabeshima, *Chem. Commun.*, 2008, 889; (*d*) M. B. Dewal, Y. Xu, J. Yang, F. Mohammed, M. D. Smith and L. S. Shimizu, *Chem. Commun.*, 2008, 3909; (*e*) R. T. Liao, W. C. Yang, P. Thanasekaran, C. C. Tsai, M. Sathiyendiran, Y. H. Liu, T. Rajendran, H. M. Lin, T. W. Tseng and K. L. Lu, *Chem. Commun.*, 2008, 3175; (*f*) R. Kusaka, Y. Inokuchi and T. Ebata, *Phys. Chem. Chem. Phys.*, 2008, **10**, 6238; (*g*) R. G. Zarracino and H. Höpfl, *Angew. Chem., Int. Ed.*, 2004, **43**, 1507.

2 (*a*) C. Ma, Q. Zhang, R. Zhang and D. Wang, *Chem.–Eur. J.*, 2006, **12**, 420; (*b*) V. Chandrasekhar and R. Thirumoorthi, *Organometallics*, 2009, **28**, 2096; (*c*) Z. H. Fard, M. R. Halvagar and S. Dehnen, *J. Am. Chem. Soc.*, 2010, **132**, 2848; (*d*) V. Chandrasekhar, K. Gopal, S. Nagendran, P. Singh, A. Steiner, S. Zacchini and J. F. Bickley, *Chem.–Eur. J.*, 2005, **11**, 5437; (*e*) V. Chandrasekhar, K. Gopal and P. Thilagar, *Acc. Chem. Res.*, 2007, **40**, 420; (*f*) M. Gielen and E. R. T. Tiekink, *Metallotherapeutic Drugs and Metal-Based Diagnostic Agents, The Use of Metals in Medicine*, 2005.

3 (*a*) V. Chandrasekhar, V. Baskar, A. Steiner and S. Zacchini, *Organometallics*, 2004, **23**, 1390; (*b*) C. Ma, Q. Li, M. Guo and R. Zhang, *J. Organomet. Chem.*, 2009, **694**, 4230; (*c*) C. Ma and J. Sun, *Dalton Trans.*, 2004, **33**, 1785; (*d*) V. Chandrasekhar, C. Mohapatra and R. J. Butcher, *Cryst. Growth Des.*, 2012, **12**, 3285.

4 (*a*) N. J. Turro, *Proc. Natl. Acad. Sci. U. S. A.*, 2005, **102**, 10766; (*b*) C. Ma, J. Sun and R. Zhang, *J. Organomet. Chem.*, 2006, **691**, 5873; (*c*) D. Braga, O. Benedi, L. Maini and F. Grepioni, *J. Chem. Soc., Dalton Trans.*, 1999, **28**, 2611; (*d*) R. Koner and I. Goldberg, *CrystEngComm*, 2009, **11**, 1217; (*e*) C. Ma, G. Tian and R. Zhang, *J. Organomet. Chem.*, 2006, **691**, 2014.

5 (*a*) H. I. Beltrán, L. S. Z. Rivera, T. Mancilla, R. Santillan and N. Farfán, *Chem.–Eur. J.*, 2003, **9**, 2291; (*b*) C. Ma, Q. Wang and R. Zhang, *Inorg. Chem.*, 2008, **47**, 7060; (*c*) R. G. Zarracino, J. R. Quiñones and H. Höpfl, *Inorg. Chem.*, 2003, **42**, 3835; (*d*) V. Chandrasekhar and R. Thirumoorthi, *Organometallics*, 2007, **26**, 5415; (*e*) J. C. Huerta, M. C. Morales, E. S. Juárez, I. F. H. Ahuactzi, J. E. García, C. G. Alcantar, J. A. G. Alvarez, H. Höpfl, H. M. Rojas and M. Sánchez, *Inorg. Chem.*, 2008, **47**, 9874.

6 (*a*) M. Gielen, *Appl. Organomet. Chem.*, 2002, **16**, 481; (*b*) E. R. T. Tiekink, *Appl. Organomet. Chem.*, 1991, **5**, 1; (*c*)

M. Gielen, H. Dalil, L. Ghys, B. Boduszek, E. R. T. Tiekink, J. C. Martins, M. Biesemans and R. Willem, *Organometallics*, 1998, **17**, 4259; (*d*) M. Gielen, M. Biesemans, R. Willem and E. R. T. Tiekink, *Eur. J. Inorg. Chem.*, 2004, **3**, 445; (*e*) V. Chandrasekhar, S. Nagendran and V. Baskar, *Coord. Chem. Rev.*, 2002, **235**, 1; (*f*) C. Ma, Y. Han, R. Zhang and D. Wang, *Dalton Trans.*, 2004, **33**, 1832.

7 (*a*) A. Bondi, *J. Phys. Chem.*, 1964, **68**, 441; (*b*) A. R. Forrester, S. J. Garden, R. A. Howie and J. L. Wardell, *J. Chem. Soc., Dalton Trans.*, 1992, **17**, 2615; (*c*) H. D. Yin, M. Hong, M. L. Yang and J. C. Cui, *J. Mol. Struct.*, 2010, **984**, 383; (*d*) C. Ma, Q. Jiang, R. Zhang and D. Wang, *Dalton Trans.*, 2003, **32**, 2975; (*e*) X. Xiao, X. Han, Z. Mei, D. Zhu, K. Shao, J. Liang, M. Tian and L. Xu, *J. Organomet. Chem.*, 2013, **729**, 28.

8 (*a*) T. P. Lockhart, W. F. Manders and E. M. Holt, *J. Am. Chem. Soc.*, 1986, **108**, 6611; (*b*) S. E. Johnson and C. B. Knobler, *Organometallics*, 1992, **11**, 3684; (*c*) D. C. Menezesa, G. M. deLimab, F. A. Carvalhob, M. G. Coelhob, A. O. Portob, R. Augusti and J. D. Ardisson, *Appl. Organomet. Chem.*, 2010, **24**, 650; (*d*) K. S. Prasad, L. S. Kumar, S. Chandan, B. Jayalakshmi and H. D. Revanasiddappa, *Spectrochim. Acta, Part A*, 2011, **81**, 276.

9 (*a*) D. Singh and J. B. Baruah, *Tetrahedron Lett.*, 2008, **49**, 4374; (*b*) D. D. Perrin, W. L. F. Armarego and D. R. Perrin, *Purification of Laboratory Chemicals*, Pergamon, Oxford, 2nd edn, 1980; (*c*) G. M. Sheldrick, *SHELXS-97, A Program for Automatic Solution of Crystal Structure*, University of Gottingen, Germany, 1997; (*d*) G. M. Sheldrick, *SHELXL-97, A Program for Crystal Structure Refinement*, University of Gottingen, Germany, 1997.